Proceedings of the Seventh (1997) International Offshore and Polar Engineering Conference
Honolulu, USA, May 25-30, 1997

ISBN 1-880653-28-1 (Set); ISBN 1-880653-31-1 (Vol. III)

Spectral Modeling of Unidirectional Nonlinear Wave Propagation Over Arbitrary Depths

S. Beji
Istanbul Technical University
Istanbul, Turkey

K. Nadaoka
Tokyo Institute of Technology
Tokyo, Japan

Abstract

A weakly-nonlinear and dispersive wave equation recently developed by the authors (Beji and Nadaoka, 1997) is used for formulating a spectral wave model describing transformations of narrow-banded unidirectional waves traveling over variable bathymetry. The performance of the model is tested against the measured data for harmonic generation over constant depth as well as nonlinear random wave propagation over varying depth. The comparisons indicate good agreement with the measurements and establish the reliability of the model. In closing, a semi-empirical dissipation term is formulated for simulating the energy loss due to breaking waves.

Key Words

Nonlinear spectral model, Varying bathymetry, Nonlinear random waves, Cnoidal waves, Stokes waves, Breaking waves.

1. Introduction

Recent years have witnessed a constantly increasing interest towards the modeling of the nonlinear aspects of ocean waves. The trend originated from the need to explain definite observations which could not be accounted for by linear models. Wave skewness related sediment transport, influence of breaking on the surf-zone processes, and effects of harmonic generation on the characteristics of a wave field are the most striking examples of such phenomena (Doering and Bowen, 1986; Nadaoka *et al.*, 1989; Kojima *et al.*, 1990). For practical applications the nonlinear wave models are not yet in common use, however, there are evidences that when augmented with appropriate generation and dissipation mechanisms, these models may well be the prototypes of the commercial models to come.

In this work a spectral model is developed using the recently introduced wave equation of Beji and Nadaoka (1997). The derivation is based on a Fourier series representation of the surface elevation with spatially varying amplitudes and phases. The resulting evolution equations are numerically solved for various test cases to demonstrate the capabilities of the model. Also, a semi-emprical dissipation term is formulated to represent energy loss due to wave breaking.

2. Wave Model and Spectral Formulation

The present work uses a nonlinear unidirectional wave equation (Beji and Nadaoka, 1997) which may be viewed as a generalized form of the Korteweg and deVries (KdV) equation:

$$C_g\eta_t + \frac{1}{2}C_p(C_p+C_g)\eta_x - \frac{(C_p-C_g)}{k^2}\eta_{xxt} - \frac{C_p(C_p-C_g)}{2k^2}\eta_{xxx} + \frac{1}{2}\left[C_p(C_g)_x + (C_p-C_g)(C_p)_x\right]\eta + \frac{3}{4}g\left(3-2\frac{C_g}{C_p}-\frac{k^2C_p^4}{g^2}\right)(\eta^2)_x = 0, \quad (1)$$

where C_p, C_g, and k are respectively the phase and group velocities and the wave-number computed according to the linear theory dispersion relation for a dominant wave frequency ω and a given local depth h, the subscripts x and t indicate partial differentiation with respect to space and time, respectively.

Unlike the KdV equation, the applicable domain of equation (1) is not restricted to only shallow waters but covers the entire range of relative depths from very shallow to infinitely deep water. For relatively shallow water waves the equation renders the KdV equation as its special case and for deep water it admits the second-order Stokes waves as solution. When the incident wave frequency coincides with the prescribed dominant frequency of the model equation the linear shoaling characteristics of the incident wave are described exactly, in accordance with the energy flux concept.

Since the form of equation (1) resembles very closely to the KdV equation it is possible to adopt all the numerical methods applicable to the KdV equation. The most straightforward approach is to use finite-difference approximations, as reported by Beji and Nadaoka (1995, 1997). Here, the so-called spectral domain formulation is employed by representing the surface displacement as a Fourier series with spatially varying harmonic amplitudes:

$$\eta(x,t) = \sum_{n=-\infty}^{+\infty} A_n(x)e^{i[\omega_n t - \int k_n(x)dx]}, \quad (2)$$

where $A_n(x)$ is the spatially varying complex wave amplitude, ω_n the radian frequency which is equal to $n\Delta\omega$, $\Delta\omega$ being the frequency of resolution. $k_n(x)$ is the spatially varying wave-number

determined according to the linear dispersion relation of equation (1) for the local depth $h(x)$ and the radian frequency ω_n:

$$C_g\omega_n - \frac{1}{2}C_p(C_p+C_g)k_n + \frac{(C_p-C_g)}{k^2}\omega_n k_n^2 - \frac{C_p(C_p-C_g)}{2k^2}k_n^3 = 0. \quad (3)$$

Substituting (2) into (1) and neglecting only the third-order spatial derivatives of $A_n(x)$ on the premise that the spatial variation of $A_n(x)$ is slow, result in the following second-order nonlinear differential equation that determines the spatial variation of each complex component:

$$i\alpha_2\frac{d^2A_n}{dx^2} + \alpha_1\frac{dA_n}{dx} + (i\alpha_0+\alpha_s)A_n = i\beta\sum_{m=-\infty}^{+\infty}(k_m+k_{n-m})A_mA_{n-m}\,e^{-i(k_m+k_{n-m}-k_n)x}, \quad (4)$$

where the free index n covers the range from $-\infty$ to $+\infty$. The coefficients are given as follows

$$\begin{aligned}
\alpha_0 &= C_g\omega_n - \frac{1}{2}C_p(C_p+C_g)k_n \\
&+ \frac{(C_p-C_g)}{k^2}\omega_n k_n^2 - \frac{C_p(C_p-C_g)}{2k^2}k_n^3, \\
\alpha_1 &= \frac{1}{2}C_p(C_p+C_g) - 2\frac{(C_p-C_g)}{k^2}\omega_n k_n \\
&+ \frac{3}{2}\frac{C_p(C_p-C_g)}{k^2}k_n^2, \\
\alpha_2 &= \left(\frac{3}{2}C_pk_n - \omega_n\right)\frac{(C_p-C_g)}{k^2}, \\
\alpha_s &= \frac{1}{2}[C_p(C_g)_x + (C_p-C_g)(C_p)_x] \\
&+ \frac{(C_p-C_g)}{k^2}\left(\frac{3}{2}C_pk_n - \omega_n\right)(k_n)_x, \\
\beta &= \frac{3}{4}g\left(3 - 2\frac{C_g}{C_p} - \frac{k^2C_p^4}{g^2}\right),
\end{aligned} \quad (5)$$

in which the spatial derivatives of k_n higher than the first have been neglected as in the wave model itself. $(k_n)_x$ appearing in α_s is computed from (3) by differentiating it with respect to x. Note that α_0 is the linear dispersion relation of the wave model and is identically zero in virtue of equation (3). However, if the wave numbers in (2) are selected as bound wave numbers then α_0 is not zero any more and it must be retained. In principle, the wavenumbers may be chosen either way, here they are selected as free wave numbers according to (3), which numerically proved to be a better choice except in the simulation of the Stokes second-order waves.

Following Bryant (1973) we multiply (4) by $-\frac{i}{\alpha_2}\exp\left(-i\frac{\alpha_1}{\alpha_2}x\right)$ so that it becomes

$$\frac{d}{dx}\left(\frac{dA_n}{dx}e^{-i\frac{\alpha_1}{\alpha_2}x}\right) = i\frac{\alpha_s}{\alpha_2}A_ne^{-i\frac{\alpha_1}{\alpha_2}x} + \beta\sum_{m=-\infty}^{+\infty}\frac{(k_m+k_{n-m})}{\alpha_2}A_mA_{n-m}\,e^{-i(k_m+k_{n-m}-k_n+\frac{\alpha_1}{\alpha_2})x}, \quad (6)$$

where α_0 has been set to zero. The spatial variations of the linear shoaling term α_sA_n and the nonlinear term A_mA_{n-m} are relatively slower and therefore these terms may be assumed locally constant, which in turn allows an integration of (6) with respect to x:

$$\frac{dA_n}{dx} = -\frac{\alpha_s}{\alpha_1}A_n + i\beta\sum_{m=-\infty}^{+\infty}\alpha_{nm}\,A_mA_{n-m}\,e^{-i(k_{n-m}+k_m-k_n)x},$$

$$\text{where} \qquad \alpha_{nm} = \frac{k_{n-m}+k_m}{\alpha_1+\alpha_2(k_{n-m}+k_m-k_n)}. \quad (7)$$

It should be remarked that the linear shoaling characteristics of the generic equation are exactly preserved in the above formulation.

Equation (7) in its present form is not suitable for numerical treatment and should be manipulated further. The summations are first re-arranged to run in the positive range only. Then, a change of variable is introduced $A_n(x) = P_n(x)\exp\left(i\int k_n dx\right)$, which removes the sine and cosine functions as in Bryant (1973). Finally, $P_n(x)$ is set to $\frac{1}{2}[a_n(x) - ib_n(x)]$ so that the evolution equations for the real variables $a_n(x)$ and $b_n(x)$ are obtained

$$\begin{aligned}
\frac{da_n}{dx} &= -\frac{\alpha_s}{\alpha_1}a_n - k_nb_n \\
&+\beta\sum_{m=1}^{N-n}\alpha_{nm}^-(a_mb_{n+m} - a_{n+m}b_m) \\
&+\frac{1}{2}\beta\sum_{m=1}^{n-1}\alpha_{nm}^+(a_mb_{n-m} + a_{n-m}b_m),
\end{aligned} \quad (8)$$

$$\begin{aligned}
\frac{db_n}{dx} &= -\frac{\alpha_s}{\alpha_1}b_n + k_na_n \\
&-\beta\sum_{m=1}^{N-n}\alpha_{nm}^-(a_ma_{n+m} + b_mb_{n+m}) \\
&-\frac{1}{2}\beta\sum_{m=1}^{n-1}\alpha_{nm}^+(a_ma_{n-m} - b_mb_{n-m}),
\end{aligned} \quad (9)$$

where

$$\alpha_{nm}^+ = \frac{k_{n-m}+k_m}{\alpha_1+\alpha_2\delta_{nm}^+}, \qquad \alpha_{nm}^- = \frac{k_{n+m}-k_m}{\alpha_1+\alpha_2\delta_{nm}^-},$$
$$\delta_{nm}^+ = k_{n-m}+k_m-k_n, \qquad \delta_{nm}^- = k_{n+m}-k_m-k_n.$$

For N number of frequency components, the free index n runs from 1 to N, resulting in $2N$ number of nonlinearly coupled first-order differential equations for the unknown components $a_n(x)$ and $b_n(x)$. Once the $a_n(x)$s and $b_n(x)$s are obtained the free surface may be constructed simply as $\eta = \Sigma a_n\cos(\omega_nt) + b_n\sin(\omega_nt)$. Various numerical integration techniques (*e.g.*, Bulirsch-Stoer, Runge-Kutta, Adams-Bashford-Moulton) are available for the integration of (8) and (9). Here, the Runge-Kutta fourth-order formulation is preferred as it proved to be the fastest while being as reliable as the other more sophisticated integration methods.

3. Numerical Simulations

The evolution equations derived in the previous section are now used for the purposes of ascertaining their reliability and exploring the capabilities of the wave model. The first case is the simulation of harmonic generation in shallow water.

3.1. Harmonic Generation in Shallow Water

Chapalain *et al.* (1992) conducted a series of experiments concerning nonlinear shallow water waves undergoing harmonic generation over constant water depth. The experiments were done for four different cases named respectively as the trial A, C, D, and H. The experimental conditions and wave parameters are given in Table 1.

Trial	h(cm)	T(s)	$\epsilon = a_0/h$	$\mu = kh$	$U_r = \epsilon/\mu^2$
A	40	2.5	0.105	0.528	0.38
C	40	3.5	0.105	0.371	0.76
D	30	2.5	0.118	0.452	0.58
H	40	3.0	0.084	0.433	0.45

Table 1

All the experiments listed in Table 1 are numerically simulated using the evolution equations given by (8) and (9). Figure 1 shows the simulated and measured harmonic components for the trials A, C, D, and H, respectively. Overall, the numerical simulations agree well with the measurements and establish confidence in the spectral model. The beat lengths are slightly underestimated; this is probably due to the limitation of the wave model to relatively narrow-banded cases. Since the third and fourth harmonics fall outside the narrow-band range of the primary wave this restriction is somewhat violated.

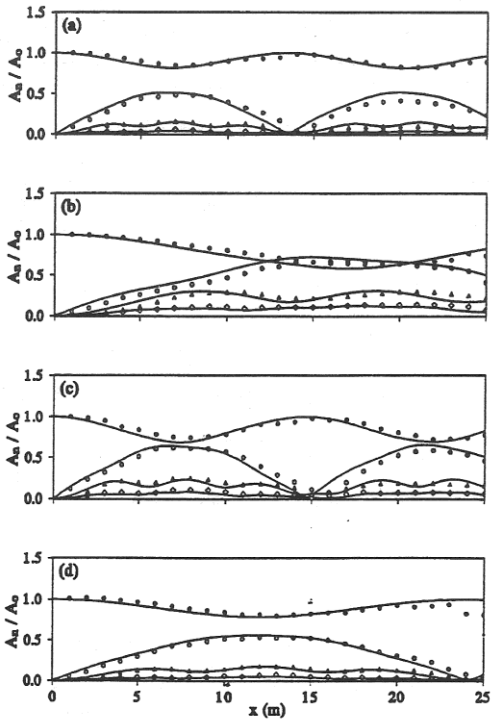

Figure 1: Experimental data of Chapalain et. al (1992) compared with the predictions of the spectral model for the trial A, C, D, and H. Scatter: experiment, solid line: computation.

3.2. Nonlinear Wave Transformations over A Submerged Bar

Nonlinear wave transformations over a submerged bar were investigated by Beji and Battjes (1993) in laboratory experiments that revealed the determining factors shaping the transformed wave spectrum. The waves were first observed to undergo harmonic generation due to nonlinear interactions in the shoaling region and then the generated bound harmonics were released behind the bar as the water depth increased again. For relatively long waves it was observed that an initially narrow-banded, sharply peaked spectrum was transformed to a broad-banded, double-peaked spectrum. On the other hand, the short wave evolutions were found to be not substantial. The details about the experimental setup and conditions can be found in Beji and Battjes (1993).

The experimental measurements for long and short sinusoidal waves and for random waves with initially JONSWAP type spectral shape are simulated using equations (8) and (9). Figures 2a and 2b show the comparisons with the experimental measurements respectively for long and short periodic waves at six different stations. The Fourier components of the recorded surface displacement at Station 1 (not shown) serves as the incoming boundary condition. In the computations five harmonic components $\omega_n = n\omega_0, n = 1, ..., 5$ were used with ω_0 corresponding to the primary wave frequency. As it is seen from the figures the model predictions agree very closely with the measurements both for the wave profiles and phases. The only exception is Station 7 of figure 2a, where obviously the narrow-bandedness of the wave model itself prevents a complete agreement.

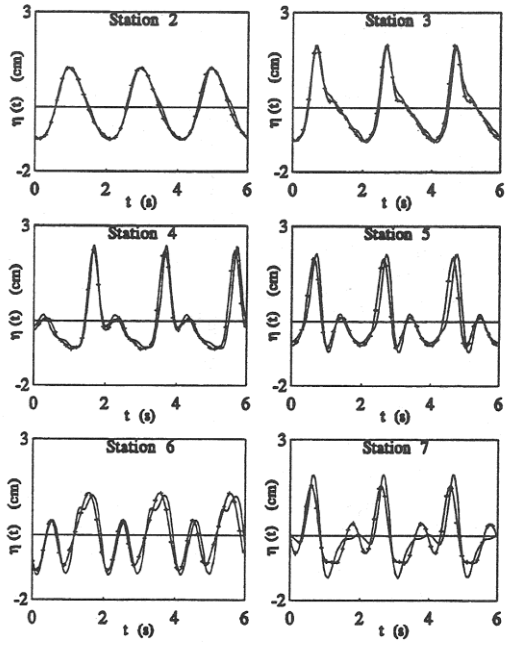

Figure 2a: Comparisons of the experimental measurements of initially sinusoidal wave propagation over a submerged bar (-) with the numerical simulations (+) for $T = 2$ s waves. Station 2: upslope 1:20, water depth 0.16 m, station 3 and 4: horizontal bottom, water depth 0.1 m, station 5: downslope 1:10, water depth 0.18 m, station 6: downslope 1:10, water depth 0.3 m, station 7: horizontal bottom, water depth: 0.4 m.

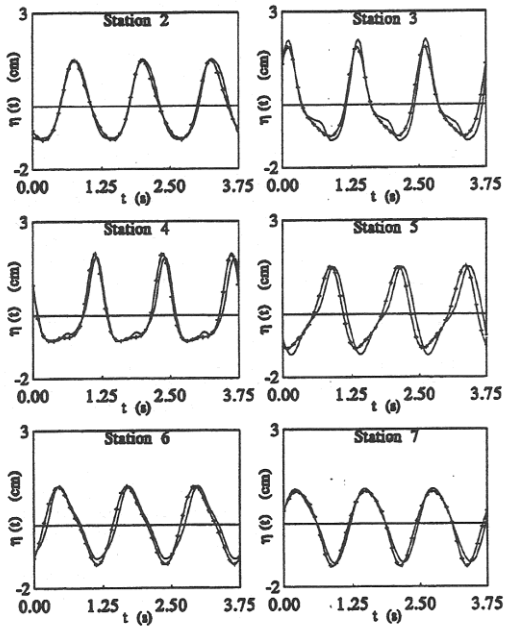

Figure 2b: Same as in figure 2a but for $T = 1.25$ s waves.

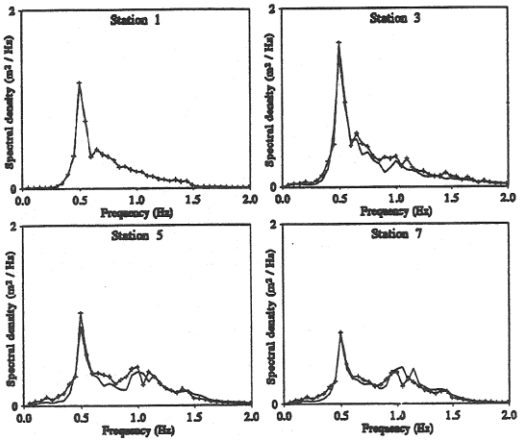

Figure 3: Comparisons of the experimental measurements (-) of the spectral evolutions over a submerged bar with the computations (+) for $T_p = 2$ s random waves.

Figures 3 and 4 depict the same comparisons for random waves having JONSWAP type incident wave spectrum with peak periods of $T_p = 2$ and $T_p = 1.25$ seconds, respectively. The records of the surface elevation at station 1 were divided into 40 segments of 512 data points and then each segment was Fourier transformed. Out of the 256 unique pairs the first 60 Fourier components, which covered a frequency range of 0.05-3.0 Hz, were found to be quite sufficient to represent the incident wave spectrum hence the spectral model was run for 40 different realizations with $N = 60$ using the measured Fourier components as the incoming boundary condition at station 1. The spectra shown in figures 3 and 4 were obtained after ensemble averaging all the realizations; no frequency averaging was done. Each spectrum has 80 degrees of freedom and 16 % normalized standard error. The overall agreement is good for both sets of measurements and the small discrepancies are attributed to the inherently narrow-banded nature of the wave model, which manifests itself as errors in the wavenumbers well outside the neigborhood of the primary wave wavenumber, which was taken to correspond to the peak period of the incident wave field.

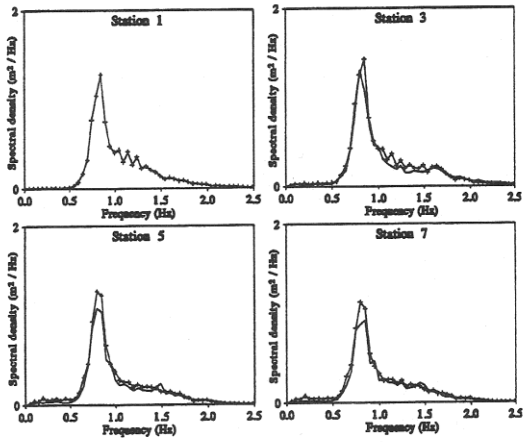

Figure 4: Same as in Figure 3 but for $T_p = 1.25$ s random waves.

4. Inclusion of Wave Breaking Effect

A semi-empirical approach is now considered to account for the dissipative role of wave breaking so as to render the spectral model operational even for breaking waves. To this end we first refer to Battjes'(1986) dissipation model for periodic waves:

$$\frac{\partial P}{\partial x} + D = 0 \quad \text{with} \quad D = \frac{D'}{cT} = \frac{B}{4\gamma^3}\frac{\rho g H^2}{T}\left(\frac{H}{h}\right)^4, \quad (10)$$

where ρ is the water density, g the gravitational acceleration, H the wave height, T the wave period, $P = EC_g$ the energy flux with $C_g = (gh)^{1/2}$ (shallow water), and B and γ the calibration parameters.

Equation (10) is applicable only to shallow water waves and it is desirable to extend it to deep water so that it will be in accord with equation (1), which is valid for arbitrary depths. Thus, we propose the following generalized form of (10) as the dissipation model

$$\frac{H_x}{H} = -\frac{B}{2\pi\gamma^3}\frac{\omega}{C_g}\left(\frac{gH}{C_p^2}\right)^4. \quad (11)$$

in which the linear shoaling term implicitly present in (10) has been removed since the wave model itself includes the linear shoaling properly. Note that instead of the term H/h in equation (10) we have introduced the term gH/C_p^2, which for shallow waters reduces to H/h. For deep water when h is very large H/h vanishes (so does the dissipation term D) and predicts no dissipation effect. On the other hand, for deep water the term gH/C_p^2 tends to kH and still predicts a non-zero dissipation due to breaking so

long as the deep water wave steepness kH is appreciable. Obviously, this feature accords well with the expectations and agrees with Miches' breaking criteria (Beji, 1995).

If the wave is represented as $a(x)\cos\phi + b(x)\sin\phi$, ϕ being the phase angle, then, according to (11), the spatial rates of reduction of the amplitude components due to breaking are

$$\frac{a_x}{a} = -\frac{B}{2\pi\gamma^3}\frac{\omega}{C_g}\left(\frac{gH}{C_p^2}\right)^4, \quad \frac{b_x}{b} = -\frac{B}{2\pi\gamma^3}\frac{\omega}{C_g}\left(\frac{gH}{C_p^2}\right)^4 \quad (12)$$

respectively for $a(x)$ and $b(x)$. Of course this formulation is true only for simple sinusoidal wave forms. The evolution equations contain not only a single component but a number of higher harmonics. It is therefore necessary to introduce some approximations to use equation (12) in (8). A plausible approach is to assume that each harmonic component is dissipated according to (12). This idea is also supported by the experimental measurements of Beji and Battjes (1993). Thus, for the wave breaking dissipation portions of (8) and (9) one can write

$$\frac{(a_n)_x}{a_n} = -\frac{B}{2\pi\gamma^3}\frac{\omega_n}{(C_g)_n}\left(\frac{gH}{C_p^2}\right)_n^4,$$
$$\frac{(b_n)_x}{b_n} = -\frac{B}{2\pi\gamma^3}\frac{\omega_n}{(C_g)_n}\left(\frac{gH}{C_p^2}\right)_n^4, \quad (13)$$

in which the wave height for each component is computed from $H_n = 2\sqrt{(a_n^2 + b_n^2)}$. Thus, the final evolution equations are

$$\frac{da_n}{dx} = -\frac{\alpha_s}{\alpha_1}a_n - k_n b_n - \frac{B}{2\pi\gamma^3}\frac{\omega_n}{(C_g)_n}\left(\frac{2gH}{C_p^2}\right)_n^4 a_n + \beta\sum_{m=1}^{N-n}\alpha_{nm}^{-}(a_m b_{n+m} - a_{n+m}b_m) + \frac{1}{2}\beta\sum_{m=1}^{n-1}\alpha_{nm}^{+}(a_m b_{n-m} + a_{n-m}b_m), \quad (14)$$

$$\frac{db_n}{dx} = -\frac{\alpha_s}{\alpha_1}b_n + k_n a_n - \frac{B}{2\pi\gamma^3}\frac{\omega_n}{(C_g)_n}\left(\frac{2gH}{C_p^2}\right)_n^4 b_n - \beta\sum_{m=1}^{N-n}\alpha_{nm}^{-}(a_m a_{n+m} + b_m b_{n+m}) - \frac{1}{2}\beta\sum_{m=1}^{n-1}\alpha_{nm}^{+}(a_m a_{n-m} - b_m b_{n-m}). \quad (15)$$

For a simple demonstration we compare the results of the numerical solution of (14) and (15) with the exact solution of equation (10) (Battjes's (1986) original model which can be solved analytically for constant depth) for the experimental measurements of Horikawa and Kuo (1966) for breaking waves over a horizontal bottom. To account for the effects of modifications made it was necessary to select a slightly different value for the parameter B. Battjes (1986) uses $B = 2$, but since always $gH/C_p^2 > H/h$ and $\sqrt{gh} > C_g$, this value gives higher dissipation rate for the generalized model. After a few trials, $B = 1$ was found to be sufficiently good. Figure 5 shows the comparisons for $h = 0.1$ m depth and $H_b/h = 0.8$ for the linearized equations, that is, when $N = 1$ in (14). The agreement with the Battjes' (1986) original model is good and supports the validity of the approximations made in deriving (12). When compared with Horikawa and Kuo's (1966) data it is clear that the model predictions fall in the range given by these authors.

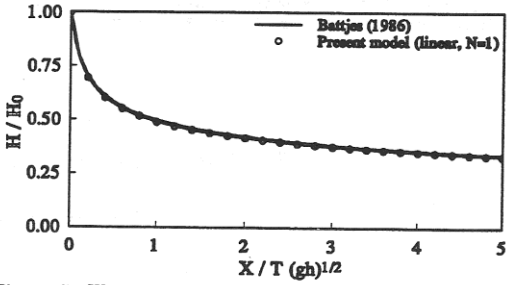

Figure 5: Wave height decay due to breaking over a horizontal bottom. The experimental conditions are from Horikawa and Kuo's (1966) measurements: $h = 0.1$ m and $H_b/h = 0.8$, H_b is the initial breaking waveheight.

5. Concluding Remarks

A spectral domain formulation of a recently developed nonlinear wave model is presented in the form of nonlinearly coupled first-order differential equations. The evolution equations describe the linear shoaling and second-order nonlinear transformations of each spectral component over arbitrary depths. Various tests are performed to check the performance of the proposed evolution equations against the measurements and the model is found to be sufficiently reliable for practical use. Furthermore, a semi-empirical formulation is suggested to account for the dissipative action of wave breaking. The proposed dissipation model works well for linear periodic waves; results for nonlinear random waves will be reported later.

References

Battjes, JA (1986). "Energy dissipation in breaking solitary and periodic waves," *Comm. on Hydraulic and Geotech. Eng.*, Internal Report, Delft Univ. of Tech., Report num. 86-5.

Beji, S (1995). "Note on a nonlinearity parameter of surface waves," *Coastal Eng.*, Vol 25, pp 81-85.

Beji, S and Battjes, JA (1993). "Experimental investigation of wave propagation over a bar," *Coastal Eng.*, Vol 19, pp 151-162.

Beji, S and Battjes, JA (1994). "Numerical simulation of nonlinear wave propagation over a bar," *Coastal Eng*, Vol 23, pp 1-16.

Beji, S and Nadaoka, K (1995). "Directional wave simulations by a time dependent nonlinear mild slope equation," *Proc. 2 nd Int Conf on Mediterranean Coastal Env*, Vol 3, pp 1929-1943.

Beji, S and Nadaoka, K (1997). "A time-dependent nonlinear mild-slope equation for water waves," *Proc. Roy. Soc. Lond. A*, Vol 453, pp 319-332.

Bryant, PJ (1973). "Periodic waves in shallow water," *J. Fluid Mech.*, Vol 59, pp 625-644.

Doering, JC and Bowen, AJ (1986). "Shoaling surface gravity waves: A bispectral analysis," *Proc 20 th Int Conf on Coastal Eng*, Vol 1, pp 150-162.

Kojima, H, Ijima, T and Yoshida, A (1990). "Decomposition and interception of long waves by a submerged horizontal plate," *Proc 22 th Int Conf on Coastal Eng*, Vol 2, pp 1228-1241.

Horikawa, K and Kuo, C-T (1966). "A study on wave transformation inside surf zone," *Proc. 10th Coastal Eng. Conf.*, Vol 1, pp 217-233.

Nadaoka, K, Hino, M and Koyano, Y (1989). "Structure of the turbulent flow field under breaking waves in the surf zone," *J Fluid Mech*, Vol 204, pp 359-387.